Modeling NO and SO_2 Oxidation by H_2O_2 in Coal-Fired Flue Gas

Sen Li[1]; Yifei Ge, Ph.D.[2]; and Xiaolin Wei[3]

Abstract: NO and SO_2 oxidization by H_2O_2 in coal-fired flue gas was modeled, and the effects of temperature and H_2O_2 concentration on NO and SO_2 oxidization were investigated. The pathways of NO and SO_2 oxidization were as follows: $H_2O_2 \rightarrow OH \rightarrow HO_2 + NO \rightarrow NO_2$ and $SO_2 + OH \rightarrow HOSO_2 + O_2 \rightarrow SO_3$, respectively. There were optimal temperature ranges of NO and SO_2 oxidization, and the ranges were 650–920 K and 650–750 K, respectively. In the optimal temperature ranges, the NO_2 conversion rate was greater than 0.9 at $MR_{H2O2/NO} > 1.9$, and the SO_3 conversion rate reached about 0.3 at $MR_{H2O2/SO2} = 0.1$–0.4. SO_2 oxidization could promote HO_2 formation to oxidize NO. **DOI: 10.1061/(ASCE)EE.1943-7870.0001458.**

Author keywords: Hydrogen peroxide; Oxidization; Nitric oxide; NO_2; SO_2.

Introduction

Nitrogen oxides (NO_x) and sulfur oxides (SO_x) are major combustion-generated pollutants from coal-fired power plants. So far the predominate postcombustion processes of De-NO_x and De-SO_x are the selective catalytic reduction (SCR) and the wet flue gas desulphurization (WFGD) respectively, which have high removal efficiencies but high operating costs (Córdoba 2015; Forzatti 2001; Li et al. 2011).

Some studies found NO could be oxidized into NO_2 in flue gas by injecting H_2O_2 (Collins et al. 2001; Myers and Overcamp 2004). Many coal-fired power plants already have WFGD for sulfur dioxide (SO_2) removal. NO_2 is much more soluble in water than NO; thus NO oxidation by injection of H_2O_2 and subsequent removal in WFGD can be an economically viable alternative to other methods of NO_x removal (Myers and Overcamp 2004; Haywood and Cooper 1998).

Cooper et al. (2002) found that the optimal temperature for NO oxidization was about 500°C by injecting H_2O_2 into flue gases, and both NO and SO_2 could be oxidized. Limvoranusorn et al. (2005) investigated the mechanisms of NO oxidization by H_2O_2, and they thought that SO_2 had some influence on NO oxidization. In order to reduce NO emission in diesel exhaust gas, Kim et al. (2001) investigated the effect of H_2O_2 on NO-to-NO_2 conversion by a detailed chemical kinetic model, but SO_2 was not considered. Actually, SO_2 concentration is high in diesel-fired gas. The composition of coal-fired flue gas is different from that of diesel-fired gas. In the meantime, the residence time of flue gas in a coal-fired boiler is much longer than that in a diesel engine; thus it requires a more complete understanding of the chemical reaction pathways for NO and SO_2 oxidization by H_2O_2.

The objective of the study is to gain a better understanding of the mechanisms of NO and SO_2 oxidization by injecting H_2O_2 into coal-fired flue gas. The effects of temperature and H_2O_2 concentration on NO on SO_2 oxidization are investigated, and the reaction pathways are provided.

Kinetic Model

Reaction Mechanism

Cantera is a suite of object-oriented software tools for problems involving chemical kinetics, thermodynamics, and/or transport processes, and it can solve the conservation equations for mass and energy in a plug flow reactor (Goodwin and Moffat 2014). In the study, Cantera code was used to model NO and SO_2 oxidization by H_2O_2 in a plug flow reactor, and the reaction pathway flux analysis was performed by MixMaster software, which is based on a conserved scalar approach to reaction fluxes (Li 2016).

The reaction mechanism included 401 reversible reactions and 73 species. The mechanism was an extension of GRI-Mech 3.0 in which the reactions of sulfur were selected from Mueller's study (Mueller et al. 2000) and to incorporate into GRI-Mech 3.0, and the mechanism included 401 reversible reactions and 73 species. The submechanism involving species containing sulfur was validated by the experiment of the effect of SO_2 on NO emission in the $CO/H_2O/O_2/NO/SO_2$ system (Mueller et al. 2000).

Model Validation of NO Oxidization by H_2O_2

In order to further validate the reaction mechanism of NO oxidization by H_2O_2, Kasper's experiment of NO oxidization by H_2O_2 was simulated in a plug flow reactor model (Kasper et al. 1996). In the experiment, the initial NO concentration was 500 ppm, N_2 gas was used as balance gas, and the residence time was 0.7 s in the reactor. The measured and simulated NO emission results are shown in Fig. 1. Although there is a difference between the simulated and measured values, the change trends of NO emission with H_2O_2 concentration are in good agreement. Therefore, the reaction

[1]Professor, State Key Laboratory of High Temperature Gas Dynamics, Institute of Mechanics, Chinese Academy of Sciences, No. 15 Beisihuanxi Rd., Beijing 100190, China (corresponding author). ORCID: https://orcid.org/0000-0002-7630-7741. Email: lisen@imech.ac.cn

[2]School of Engineering Science, Univ. of Chinese Academy of Sciences, Beijing 100190, China. Email: geyifei@imech.ac.cn

[3]Professor, State Key Laboratory of High Temperature Gas Dynamics, Institute of Mechanics, Chinese Academy of Sciences, No. 15 Beisihuanxi Rd., Beijing 100190, China. Email: xlwei@imech.ac.cn

Note. This manuscript was submitted on December 18, 2017; approved on May 15, 2018; published online on September 4, 2018. Discussion period open until February 4, 2019; separate discussions must be submitted for individual papers. This paper is part of the ***Journal of Environmental Engineering***, © ASCE, ISSN 0733-9372.

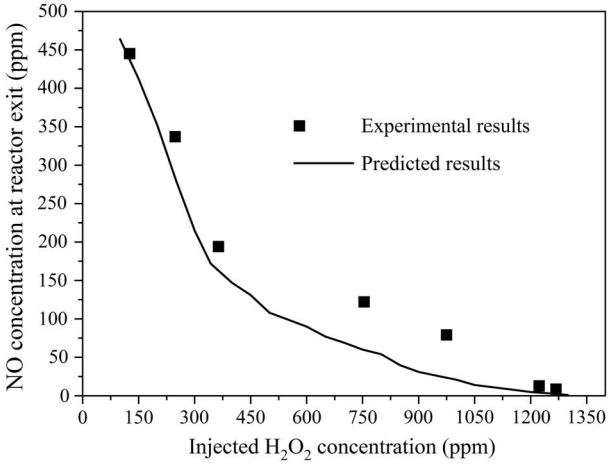

Fig. 1. Comparison of the experimental and predicted NO emission.

Table 1. Compositions of coal-fired flue gas

Species	Concentration (% by volume)
CO_2	14.96
H_2O	6.55
O_2	2.89
N_2	75.49
SO_2	0.11
NO	0.08
CO	0.005

mechanism can be used to analyze the influencing mechanism of NO oxidization by H_2O_2.

Simulation Conditions

In the simulation of NO and SO_2 oxidation by H_2O_2, an adiabatic system of a plug flow reactor model is used to model NO oxidization in coal-fired flue gas at constant pressure (1.01 bar), and the residence time of flue gas reactions is 0.4 s. A typical Chinese coal is selected as fuel, and the main compositions of coal-fired flue gas are presented in Table 1, where some trace compositions are ignored in the study.

In order to investigate the effect of the H_2O_2 injection amount on NO and SO_2 oxidation, the molar ratio of H_2O_2 to NO ($MR_{H2O2/NO}$) and the molar ratio of H_2O_2 to SO_2 ($MR_{H2O2/SO2}$) are respectively defined as

$$MR_{H2O2/NO} = C_{0,H2O2}/C_{0,NO} \quad (1)$$

$$MR_{H2O2/SO2} = C_{0,H2O2}/C_{0,SO2} \quad (2)$$

where $C_{0,NO}$, $C_{0,SO2}$, and $C_{0,H2O2}$ = initial concentrations of NO, SO_2, and H_2O_2 in flue gas, respectively.

Simulation Results and Discussion

Effects of Temperature and H_2O_2 Concentration on NO and SO_2 Oxidization

Fig. 2 shows the variations of SO_x and NO_x with the residence time in the plug flow reactor. The results indicate that, with the increase of residence time, H_2O_2 concentration in flue gas decreases, NO and SO_2 are respectively oxidized into NO_2 and SO_3, and the

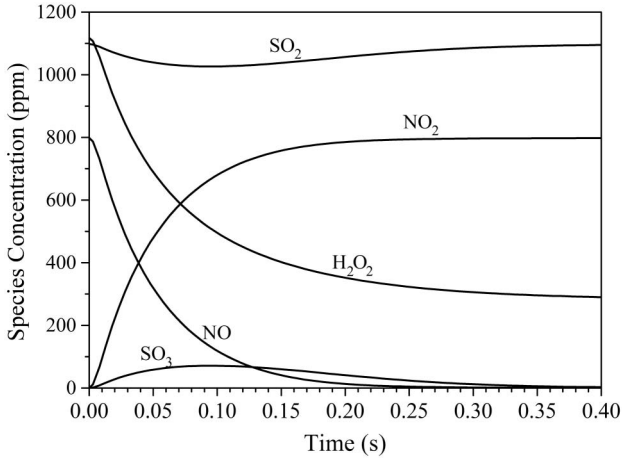

Fig. 2. Concentration variations of SO_x and NO_x with the residence time in the plug flow reactor at $C_{0,H2O2} = 1{,}120$ ppm, $C_{0,SO2} = 1{,}100$ ppm, $C_{0,NO} = 800$ ppm, and $T = 750$ K.

consumptions of NO and SO_2 coincide with the formations of NO_2 and SO_3 as follows:

$$C_{0,NO}–C_{t,NO} = C_{t,NO2} \quad (3)$$

$$C_{0,SO2}–C_{t,SO2} = C_{t,SO3} \quad (4)$$

where, $C_{t,NO}$, $C_{t,NO2}$, $C_{t,SO2}$, and $C_{t,SO3}$ = concenrations of NO, NO_2, SO_2, and SO_3 at residence time t.

Compared to SO_2, NO is easily oxidized (Fig. 2). At the reactor outlet (i.e., at $t = 0.4$ s), the conversion rates of NO_2 and SO_3 (CR_{NO} and CR_{SO2}) are respectively defined as

$$CR_{NO2} = C_{0.4,NO2}/C_{0,NO} \quad (5)$$

$$CR_{SO3} = C_{0.4,SO3}/C_{0,SO2} \quad (6)$$

Fig. 3 shows the effects of H_2O_2 and temperature on the conversion rates of NO_2 and SO_3. As Fig. 3(a) shows, at a given $MR_{H2O2/NO}$, with the increase of temperature, the NO_2 conversion rate first rises to a peak value and then falls; thus the temperature has an optimal range. With the increase of $MR_{H2O2/NO}$, the optimal range of temperature becomes wide, and the NO_2 conversion rate is greater than 0.9 at $MR_{H2O2/NO} > 1.9$ and $T = 650$–920 K.

In the practical tail flue gas duct of a coal-fired utility boiler, the temperature of flue gas is in the optimal temperature range, H_2O_2 can be injected at 920 K, NO is first effectively oxidized, and subsequently SO_2 is oxidized with the decease of flue gas temperature. H_2O_2 can be rapidly and efficiently consumed, and injecting H_2O_2 has no effect on the heating surface of the boiler. For storage and transportation safety, in industrial applications, usually, H_2O_2 concentration is 30%.

As Fig. 3(b) shows, the SO_3 conversion rate can reach about 0.3 at $MR_{H2O2/SO2} = 0.1$–0.4 and $T = 650$–750 K, and the SO_3 conversion rate is obviously less than the NO_2 conversion rate. The optimal temperature range of SO_2 oxidization is narrower than that of NO_2 oxidization, SO_2 is easy to oxidize at a lower temperature, and increasing the H_2O_2 amount at $MR_{H2O2/SO2} > 0.4$ is not conducive to SO_2 oxidization.

In order to understand the mechanism of NO_2 oxidization by H_2O_2, the normalized sensitivity of NO_2 concentration toward reactions is calculated. The sensitivity analysis coefficients are obtained through the perturbation of the pre-exponential factor A

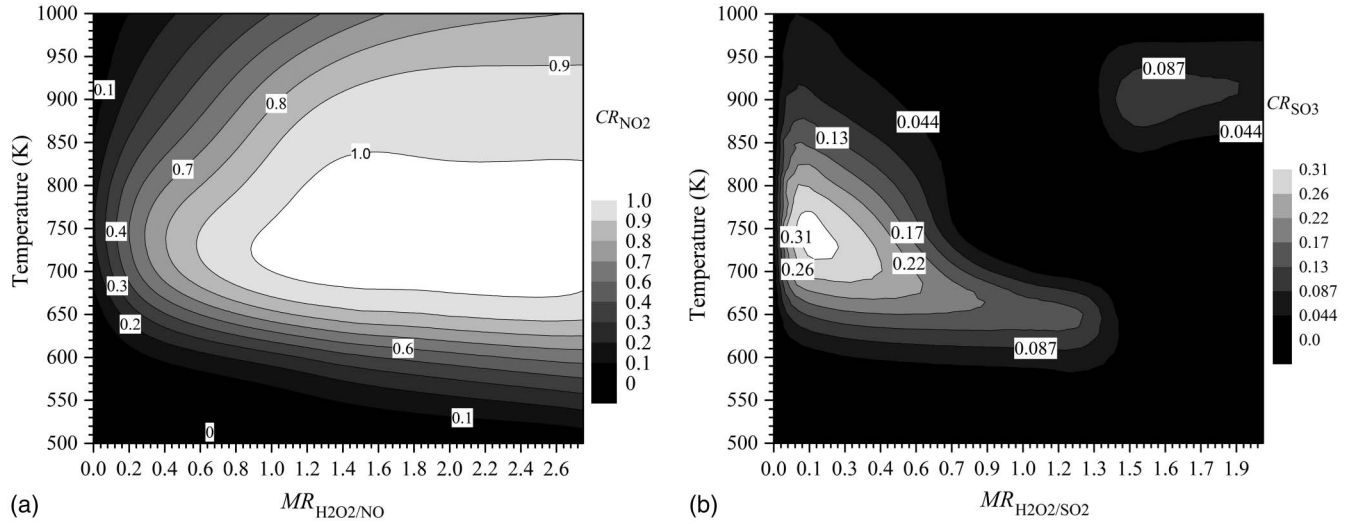

Fig. 3. Effects of H_2O_2 and temperature on the conversion rates of NO_2 and SO_3 at the reactor outlet.

in the Arrhenius equation of reactions, and the normalized sensitivity coefficient (S_j) is defined as

$$S_i = \frac{\partial \ln c}{\partial \ln k_i} \tag{7}$$

where $c = NO_2$ concentration; and k_i = pre-exponential factor A in the Arrhenius equation of the reaction i. The value of the sensitivity coefficient indicates a positive or negative influence on c by k_i, a positive value means that the value of c increases as k_i increases, and a negative value means that the value of c decreases as k_i increases. The reason for the high value of the coefficient is that the reaction is the key chain branching step and strongly promotes NO_2 formation.

As Fig. 4 shows, the normalized sensitivity coefficients of R1–R4 are the top four reactions, and it means these four reactions are most important for NO_2 formation. They are

$$H_2O_2(+M) = 2\,OH(+M) \tag{R1}$$

$$OH + H_2O_2 = HO_2 + H_2O \tag{R2}$$

$$HO_2 + NO = NO_2 + OH \tag{R3}$$

$$HO_2 + OH = O_2 + H_2O \tag{R4}$$

Since the values of the sensitivity coefficients of R1, R2, and R3 reactions are positive, it means that above three reactions are conducive to NO_2 formation, and the OH free radical plays an important role for the formation HO_2. As R4 demonstrates, free radicals of OH and HO_2 are consumed, which inhibits NO oxidization.

In order to investigate the NO oxidization reaction mechanism, a reaction pathway flux analysis was performed using MixMaster code (a Python program that is part of the Cantera suite), and the integral path analysis was based on a conserved scalar approach to reaction fluxes (Goodwin et al. 2017). Fig. 5 illustrates the schematic diagram of reaction pathways for O-containing species at $t = 0.16$ s.

As Fig. 5 shows, a part of H_2O_2 first decomposes into a free radical OH by R1, the remnant H_2O_2 reacts with OH to form HO_2 by R2, and then NO is oxidized by HO_2 through R3. The reaction pathways of NO oxidization are as follows: $H_2O_2 \rightarrow OH \rightarrow HO_2 + NO \rightarrow NO_2$. In the above reaction pathways, the free radicals of OH and HO_2 are crucial to NO oxidization, and OH promotes HO_2 formation to oxidize NO.

Fig. 6 shows the effect of temperature on the HO_2 free radical. With the increase of temperature, HO_2 concentration first increases

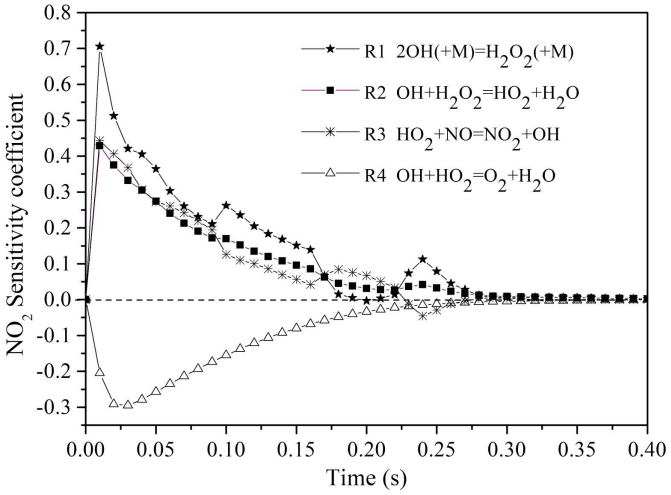

Fig. 4. Sensitivity of NO_2 concentrations toward the most important reactions at $C_{0,H202} = 1{,}120$ ppm, $C_{0,NO} = 800$ ppm, $C_{0,SO2} = 1{,}100$ ppm, and $T = 750$ K.

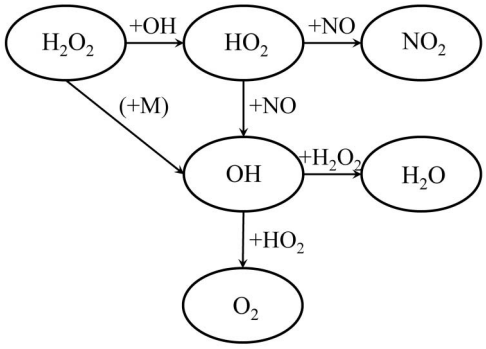

Fig. 5. Schematic diagram of reaction pathways for O-containing species in plug flow reactor at $t = 0.16$ s ($C_{0,H202} = 1{,}120$ ppm, $C_{0,NO} = 800$ ppm, $C_{0,SO2} = 1{,}100$ ppm).

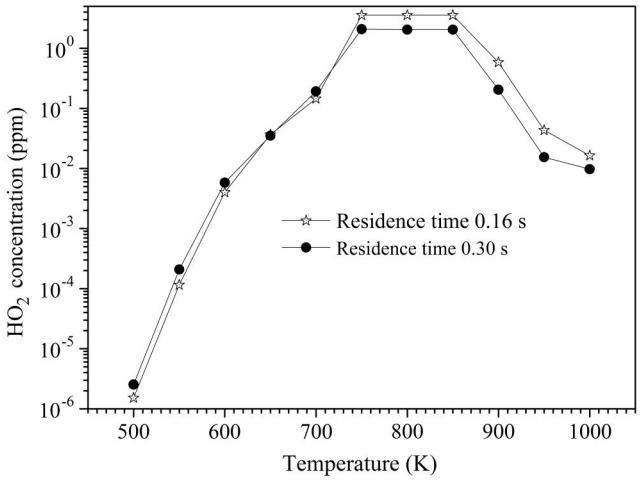

Fig. 6. Effect of temperature on free radical of HO_2 at $C_{0,H202} = 1{,}120$ ppm, $C_{0,NO} = 800$ ppm, and $C_{0,SO2} = 1{,}100$ ppm.

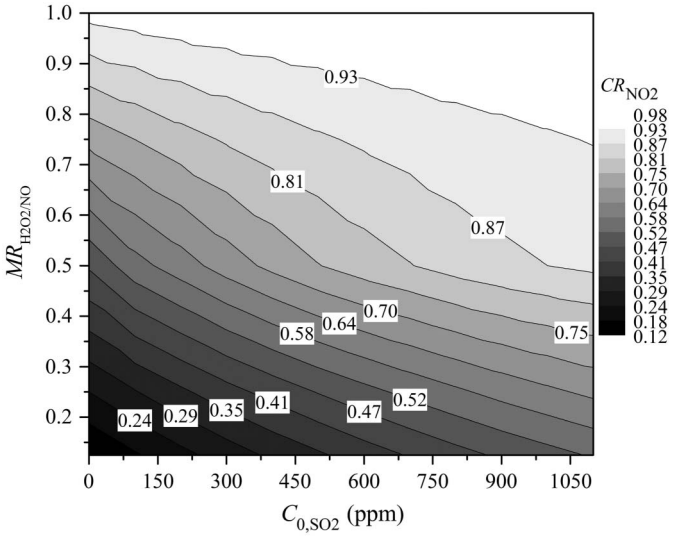

Fig. 7. Effect of H_2O_2 and SO_2 on NO conversion rate at $T = 750$ K.

at 500–750 K, then almost keeps constant at 750–850 K, and finally decreases at above 850 K. At 650–920 K, HO_2 concentration is high, and thus NO_2 conversion rate can be obtained, as shown in Fig. 3(a). Since OH concentration is low at low temperature (500–750 K), increasing the temperature can enhance OH formation to promote NO oxidization by R1, R2, and R3. However, when the temperature reaches above 850 K, a high concentration of OH enhances HO_2 consumption to inhibit NO oxidization reaction by R4.

Effects of SO_2 Concentration on NO Conversions

In order to analyze the effect of SO_2 on NO oxidization by H_2O_2, NO emission at the plug flow reactor outlet is investigated at 750 K, and the simulation result is shown in Fig. 7. The NO_2 conversion rate increases with the increase of H_2O_2 and SO_2 concentrations. When $C_{0,SO2}$ increases from 0 to 1,100 ppm, CR_{NO2} increases from 0.18 to 0.57 at $MR_{H2O2/NO} = 0.2$, and it increases from 0.75 to 0.93 at $MR_{H2O2/NO} = 0.8$. Thus, at low H_2O_2 concentration, the increase of initial SO_2 concentration has a notable influence on the NO_2 conversion rate (Fig. 7).

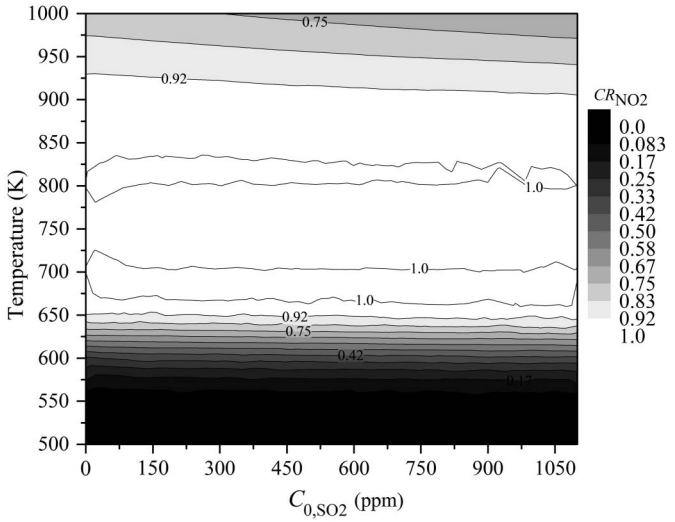

Fig. 8. Effect of temperature and SO_2 on NO oxidization at $MR_{H2O2/NO} = 1.75$.

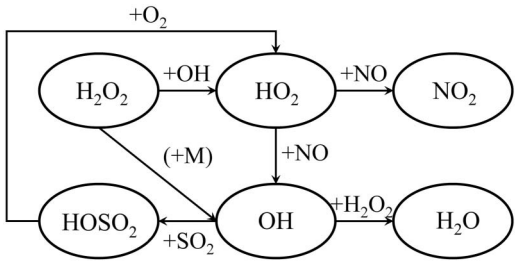

Fig. 9. Schematic diagram of reaction pathways for O-containing species at $t = 0.3$ s and $T = 750$ K.

Fig. 8 shows the effects of initial SO_2 concentration and temperature on NO oxidization at high $MR_{H2O2/NO}$. Compared to temperature, SO_2 concentration has a negligible influence on the NO_2 conversion rate at high $MR_{H2O2/NO}$. Thus, temperature has a dominant effect on NO oxidization at high H_2O_2 concentration, and the NO_2 conversion rate can reach above 0.9 at $T = 650$–925 K.

In order to analyze the influence mechanism of SO_2 on NO oxidization by H_2O_2 at low $MR_{H2O2/NO}$, the reaction pathways of O-containing species in a plug flow reactor at $t = 0.3$ s are presented in Fig. 9. Compared to Fig. 5, Fig. 9 indicates that, at low $MR_{H2O2/NO}$, SO_2 enhances HO_2 formation to oxidize NO by the following reactions:

$$SO_2 + OH = HOSO_2 \quad \text{(R5)}$$

$$HOSO_2 + O_2 = HO_2 + SO_3 \quad \text{(R6)}$$

The competitive reactions between R4 and R5 inhibit HO_2 consumption, and R6 promotes HO_2 formation to oxidize NO through R3. In the meantime, SO_2 is oxidized through R5 and R6, and the reaction pathways of SO_2 oxidization are as follows: $SO_2 + OH \rightarrow HOSO_2 + O_2 \rightarrow SO_3$.

Fig. 10 shows the effect of SO_2 concentration on the free radicals of OH and HO_2 at low $MR_{H2O2/NO}$. With the increase of SO_2 concentration, OH concentration decreases by R5 [Fig. 10(a)], HO_2 concentration increases by R6 [Fig. 10(b)], and finally NO oxidization is promoted by R3 (Fig. 7).

J. Environ. Eng., 2018, 144(11): 04018113

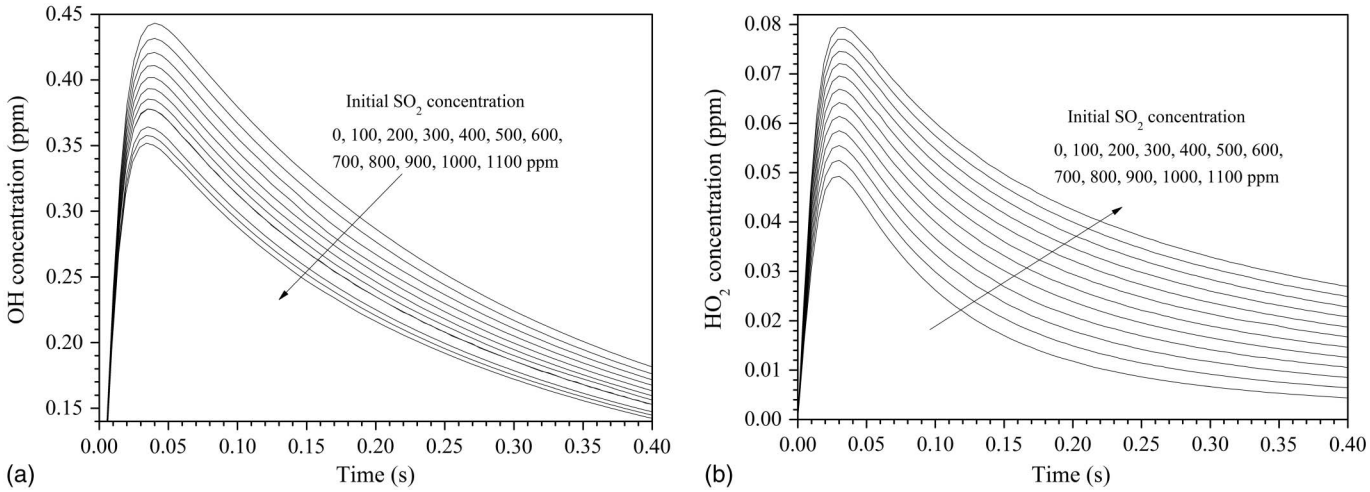

Fig. 10. Effects of initial SO_2 concentration on OH and HO_2 at $C_{0,H202} = 200$ ppm and $T = 750$ K.

At high H_2O_2 concentration, the reactions of R1 and R2 are controlled by temperature; thus increasing temperature can effectively promote HO_2 formation to oxidize NO by R1–R3 (Fig. 8).

Conclusions

NO and SO_2 oxidization by H_2O_2 in coal-fired flue gas was simulated, and the effects of temperature and H_2O_2 concentration on SO_3 and NO_2 conversion rates were investigated. There are optimal temperature ranges of NO and SO_2 oxidization, and they are 650–920 K and 650–750 K, respectively. Increasing $MR_{H2O2/NO}$ makes the optimal temperature range of the NO_2 conversion rate become wide. In the optimal temperature ranges, the NO_2 conversion rate is greater than 0.9 at $MR_{H2O2/NO} > 1.9$, and the SO_3 conversion rate can reach about 0.3 at $MR_{H2O2/SO2} = 0.1$–0.4. The SO_3 conversion rate is obviously less than the NO_2 conversion rate, and SO_2 is easy to oxidize at a lower temperature. The reaction pathways of NO and SO_2 oxidization were as follows: $H_2O_2 \rightarrow OH \rightarrow HO_2 + NO \rightarrow NO_2$ and $SO_2 + OH \rightarrow HOSO_2 + O_2 \rightarrow SO_3$, respectively.

Acknowledgments

Financial support by the National Natural Science Foundation of China (No. 51376189) and National Key Research and Development Plan of China (No. 2016YFB0601503) are acknowledged.

References

Collins, M. M., C. D. Cooper, J. D. Dietz, C. A. Clausen III, J. D. Dietz, and L. M. Tazi. 2001. "Pilot-scale evaluation of H_2O_2 injection to control NO_x emissions." *J. Environ. Eng.* 127 (4): 329–336. https://doi.org/10.1061/(ASCE)0733-9372(2001)127:4(329).

Cooper, C. D., C. A. Clausen, and L. Pettey. 2002. "Investigation of ultraviolet light-enhanced H_2O_2 oxidation of NO_x emissions." *J. Environ. Eng.* 128 (1): 68–72. https://doi.org/10.1061/(ASCE)0733-9372(2002)128:1(68).

Córdoba, P. 2015. "Status of flue gas desulphurisation (FGD) systems from coal-fired power plants: Overview of the physic-chemical control processes of wet limestone FGDs." *Fuel* 144 (15): 274–286. https://doi.org/10.1016/j.fuel.2014.12.065.

Forzatti, P. 2001. "Present status and perspectives in de-NO_x SCR catalysis." *Appl. Catal. A-Gen.* 222 (1–2): 221–236. https://doi.org/10.1016/S0926-860X(01)00832-8.

Goodwin, D. G. N., H. K. Moffat, and R. L. Speth. 2017. "Cantera: An object-oriented software toolkit for chemical kinetics, thermodynamics, and transport processes." Accessed May 20, 2017. https://www.cantera.org.

Goodwin, D. M. N., and H. S. R. Moffat. 2014. "Cantera: A suite of object-oriented software tools for problems involving chemical kinetics, thermodynamics, and/or transport processes." Accessed Mar 15, 2017. https://sourceforge.net/projects/cantera.

Haywood, J. M., and C. D. Cooper. 1998. "The economic feasibility of using hydrogen peroxide for the enhanced oxidation and removal of nitrogen oxides from coal-fired power plant flue gases." *J. Air Waste Manage.* 48 (3): 238–246. https://doi.org/10.1080/10473289.1998.10463679.

Kasper, J. M., C. A. Clausen, and C. D. Cooper. 1996. "Control of nitrogen oxide emissions by hydrogen peroxide-enhanced gas-phase oxidation of nitric oxide." *J. Air Waste Manage.* 46 (2): 127–133. https://doi.org/10.1080/10473289.1996.10467444.

Kim, I., J. Park, and S. Goto. 2001. *Conversion of nitric oxide to nitrogen dioxide using hydrogen peroxide*. SAE Technical Paper Rep. No. 2000-01-1931. Warrendale: SAE International.

Li, J., H. Chang, J. Hao, L. Ma, and R. T. Yang. 2011. "Low-temperature selective catalytic reduction of NO_x with NH_3 over metal oxide and zeolite catalysts—A review." *Catal. Today* 175 (1): 147–156. https://doi.org/10.1016/j.cattod.2011.03.034.

Li, S. 2016. "Modeling of pressure effects on flame structure and soot formation of n-heptane/air co-flow laminar flames by skeletal reaction mechanism." *Appl. Therm. Eng.* 106 (5): 1458–1465. https://doi.org/10.1016/j.applthermaleng.2016.03.006.

Limvoranusorn, P., C. D. Cooper, and J. D. Dietz. 2005. "Kinetic modeling of the gas-phase oxidation of nitric oxide using hydrogen peroxide." *J. Environ. Eng.* 131 (4): 518–525. https://doi.org/10.1061/(ASCE)0733-9372(2005)131:4(518).

Mueller, M. A., R. A. Yetter, and F. L. Dryer. 2000. "Kinetic modeling of the $CO/H_2O/O_2/NO/SO_2$ system: Implications for high-pressure fall-off in the $SO_2 + O(+M) = SO_3(+M)$ reaction." *Int. J. Chem. Kinet.* 32 (6): 317–339. https://doi.org/10.1002/(SICI)1097-4601(2000)32:6<317::AID-KIN1>3.0.CO;2-L.

Myers, J. E. B., and T. J. Overcamp. 2004. "Hydrogen peroxide scrubber for the control of nitrogen oxides." *Environ. Eng. Sci.* 19 (5): 321–327. https://doi.org/10.1089/10928750260418953.